Polymer 41 (2000) 4579–4587

polymer

Crystallisation of blends of LLDPE with branched VLDPE

R.A. Shanks*, G. Amarasinghe

Department of Applied Chemistry, RMIT University, Melbourne, Victoria 3001, Australia

Received 8 March 1999; received in revised form 7 September 1999; accepted 15 September 1999

Abstract

Blends of linear low-density polyethylene (LLDPE) and very low-density polyethylene (VLDPE) with long chain branching have been prepared by extrusion mixing. All copolymers have similar branch lengths and are commercial ethylene–octene copolymers. The copolymers and blends were subjected to crystallisation ("thermal fractionation") by stepwise cooling interspersed with isothermal periods and the fractionated samples were examined by differential scanning calorimetry (DSC). Thermal fractionation by DSC separates copolymers and blends according to their branching densities. Thermal fractionation data were used to calculate branching distribution in polyethylenes using calibration curves obtained from the literature. It is found that LLDPE contains a broad distribution of branching densities whereas the VLDPEs contain a narrow distribution, though with shorter average lengths between branches. Where both polymers have common melting endotherms in the thermally fractionated blends they may co-crystallise if they are mutually miscible in the melt. In blends containing low amounts of VLDPEs, the branching observed are combined effects of each individual polymer indicating that polymers retain some of their individual features after blending. The blends with high VLDPE amounts show some miscibility in the melt suggesting co-crystallisation between the copolymers may be occurring. © 2000 Elsevier Science Ltd. All rights reserved.

Keywords: Polyethylene blends; Thermal fractionation; Crystallisation

1. Introduction

Linear low-density polyethylene (LLDPE) is used in many film applications where flexibility, toughness and strength are required in a polyethylene film. Although LLDPEs have superior mechanical properties [1], which enable very thin gauge films to be produced, they exhibit poor processability due to the presence of short chain branches [2]. Conversely, low-density polyethylene (LDPE) is easier to process, and in particular it has higher melt strength. The superior melt strength of LDPE arises from the presence of long chain branching and long chain branches are thought to provide more entanglements within the melt. Blending LDPE up to 20% (w/w) proportions with LLDPE provides a better level of long chain branching retaining some of the properties of LLDPE [3]. Another improved feature of blending LDPE into LLDPE is the better transparency of LLDPE–LDPE films.

The development of single-site catalyst technology has enabled production of a new range of polyethylenes including very low-density polyethylene (VLDPE) [4,5]. VLDPE has more long branches than conventional LLDPE and these branches are more evenly distributed along the polymer due to the selectivity of the metallocene catalyst used in the polymerisation. The VLDPE, which also has long branches, will be similar to LDPE except those short branches will be better defined in number and distribution. Metallocene polyethylenes are also found to have lower haze than LDPE and processability similar to LDPE [6]. Thus, blending VLDPE into conventional LLDPE is expected to improve properties and performance including melt tension and transparency in the LLDPE blends.

Polyethylene copolymers, produced using both conventional Ziegler–Natta polymerisation catalysts and single-site or metallocene catalysts, have been found to exhibit structural heterogeneity due to the unequal reactivities of ethylenes and the 1-olefin comonomer [7–16]. Differential scanning calorimetric (DSC) analysis of these copolymers showed broad or several melting peaks suggesting uneven branching in these copolymers [9–19]. The most common methods used for the analysis of structural heterogeneity are fractionation methods such as solvent gradient elution fractionation (SGEF, direct extraction by solvents/non-solvent mixtures; fractionation mainly based on the molecular weight differences) and temperature rising elution fractionation (TREF, crystallisation/dissolution procedures; fractionation based on the differences in crystallinity) [16]. Due

---

* Corresponding author. Tel.: +61-3-9925-2122; fax: +613-9925-2122.
E-mail address: shanksra@rmit.edu.au (R.A. Shanks).

PII: S0032-3861(99)00678-3

Table 1
Details of the polymers used in this research

Code[a]	Comonomer %	MFI (g/10 min)	Density (g/cm^3)
LLDPE	5.0	0.94	0.927
VLDPE1	7.5	1.0	0.915
VLDPE2	9.5	1.0	0.908

[a] All data were taken from data sheets published by the manufacture.

to the lengthy steps and high cost involved, these procedures are not widely used for the compositional analysis of polymers.

Alternative fractionation methods such as stepwise annealing [20], stepwise isothermal crystallisation [20–31] and successive self-nucleation/annealing [32–34], etc. by differential scanning calorimetry have been reported. We have recently examined a stepwise cooling program to fractionate polymers [26]. In this method, the polymer is quickly cooled to the desired crystallisation temperature from the melt and then successively held for a certain time at decreasing temperatures. At each cooling step, all molecules, which can crystallise, have time to do so and molecules or segments of molecules are separated based on branching density. In fact, Adisson et al. [25] showed that the DSC thermograms of thermally treated samples of LLDPEs and combined TREF fractions were almost the same indicating that this DSC fractionation proceeded mainly according to the branching not to the molar mass. Hence, this process is termed thermal fractionation.

Thermal fractionation does not physically separate the polymer sample into fractions, but rather the crystals within the sample are separated into groups of lamellae of different thicknesses depending on the extent and distribution of branching. According to the exclusion model [23,24,35], crystallites of copolymers are formed from the crystallisable and non-crystallisable components. During crystal growth, crystallisable units continuously grow attaching to the lamella surface whereas non-crystallisable units are excluded thereby hindering the lamellae thickening. The fold period will thus depend on the frequency of the non-crystallisable units such as short branches and branch points of long branches along the copolymer chain. The exclusion of branch points from crystals should be complete due to the long equilibration (50 min) at each isothermal crystallisation temperature. Since short branches (except methyl [36]) and branch points of long branches are excluded from the crystal, it is possible to obtain a distribution of lamellae, which also represents the branching distribution of polymers. In particular, DSC fractionation based on stepwise slow crystallisation carried out at progressively lower temperatures from the melt can be considered closer to equilibrium conditions. Therefore, the subsequent melting of the fractionated sample in the DSC reveals information about the lamella thickness distribution and the DSC data can be used to determine the chemical composition distribution of copolymers [23–25,31,34].

While the commercial outcomes of metallocene polyethylene blends may be important our long-term goal is to understand the microstructure of these copolymers and their blends to extend the theories of polymer–polymer miscibility and the role of microstructure on properties and performance. In our efforts to investigate metallocene or single-site catalysed grade polyolefin blends, we have studied blends of LLDPE with VLDPE. Here, we present the application of a thermal fractionated crystallisation method to study the branching distributions and melt miscibility of the copolymers and their blends.

2. Experimental

2.1. Materials

The polyethylenes used in this study are commercial 1-octene copolymers and have similar branch length. The LLDPE is a Ziegler–Natta solution/slurry polymerised type and the VLDPEs are single-site-polymerised types with long chain branches, obtained from Dow Plastics, Australia. The details of the polymers used are shown in Table 1.

2.2. Preparation of blends

The pellets of each VLDPE1 and VLDPE2 were mixed with LLDPE in various proportions (by weight) 10, 20, 50 and 80%. The uniformly mixed pellets were fed into an Axon BX-12 extruder (Axon Australia Pty. Ltd., Australia) with a Gateway screw, 12.5 mm diameter and a length:diameter of 26:1. The temperature profile of the extruder was 120, 180, 180 and 150°C at the feed zone, compression zone, metering zone and die-end, respectively. The screw speed was 40 rpm. The extruded strands were passed through room temperature water and subsequently granulated after drying in air. The blends are labelled by the VLDPE content; 10% VLDPE1 blend contains 10% of VLDPE1 by weight.

2.3. Differential scanning calorimetry

Thermal fractionation and thermal analyses were performed on a Perkin–Elmer series Pyris1 differential scanning calorimeter with Pyris software version 3.0. The DSC was operated at ambient temperature mode with a cold finger cooled to 1–5°C with ice/water and under a nitrogen blanket (N_2 flow 20 ml/min). Samples weighing about 2–5 mg (Perkin–Elmer AD-2Z Autobalance) were sealed in crimped aluminium pans. About 3–4 mm long pieces were cut from the strands of melt-mixed blends and vertically cut thin slices were obtained from pellets of neat polymers.

Table 2
Branching and proportion of polymer in each fraction for pure polymers and their blends

T_m (°C)	Branches/ 1000 C	LLDPE 100%	VLDPE1 100%	VLDPE2 100%	VLDPE1 10%	VLDPE1 20%	VLDPE1 50%	VLDPE1 80%	VLDPE2 10%	VLDPE2 20%	VLDPE2 50%	VLDPE2 80%
125	4	23.2			25.5	21.4	14.0	2.5	23.8	22.0	11.9	4.7
119	7	11.9			8.2	7.7	6.7	6.4	8.2	7.2	5.4	3.0
115	9	11.1			11.4	12.5	15.7	15.1	12.1	10.0	6.6	4.1
111	10	11.7	49.5		13.0	15.2	21.1	27.6	13.4	12.2	13.3	15.7
107	12	10.2	12.1	38.3	11.6	11.6	12.8	14.5	10.4	11.5	16.8	21.4
103	14	8.8	10.4	12.4	9.1	9.1	9.9	10.6	8.8	9.4	11.7	12.9
99	16	6.9	9.1	8.6	6.8	7.5	7.6	8.5	7.1	7.7	9.2	10.3
95	18	6.4	7.9	8.5	5.7	6.1	5.7	6.6	5.7	6.3	8.0	8.9
91	20	5.3	6.3	7.7	3.8	4.9	3.8	4.9	4.3	5.5	7.0	7.6
87	21	4.5	4.8	6.9	2.9	3.8	2.7	3.2	3.5	4.6	5.4	6.2
83	23			6.1	2.0				2.8	3.8	4.6	5.1
80	25			5.8							3.7	4.3
76	27			5.7								

2.4. Standard DSC analysis

The previous thermal effects were removed by melting the samples to 180°C and holding at 180°C for 5 min. The samples were then cooled to 30°C to obtain the crystallisation temperature (T_c) and heated again to 150°C to obtain the peak melting temperature (T'_m). A cooling and heating rate of 10°C/min was used. A baseline was run with a similar empty pan using the same methods. Peak area and temperatures were determined following the calibration with an indium standard.

2.5. Thermal fractionation method

The samples were melted at 180°C for 5 min and then cooled to 122°C at a nominal rate of 200°C/min. Isothermal crystallisation was continued for 50 min at 122°C. The sample was cooled to 118°C at a 200°C/min rate and another isothermal crystallisation followed. This procedure was repeated in every 4°C step until 46°C and the sample was cooled to room temperature at a 200°C/min rate. The melting scans were obtained by heating the thermal fractionated samples from 30 to 150°C at a 10°C/min heating rate.

2.6. Data analysis

The specific heat was calculated by using the multiple curve method on raw heat flow data. The degree of branching (B) and degree of crystallinity (χ_c) were calculated from calibration curves derived from TREF results of previous researchers [10]. The relationships between peak melting temperatures (T_m), B and χ_c were $T_m = -2.18B + 134$ and $\chi_c = -2.51B + 0.86$, respectively. The degree of branching is reported as the number of branches per 1000 backbone carbon atoms. The amount of polymer in each fraction (Table 2) was then estimated using the calculated crystallinity values and area under each endotherm (A); $\%\text{Polymer} = (A/\%\chi_c) \times 100$.

3. Results and discussion

Fig. 1 shows the specific heat curve for LLDPE after thermal fractionation. The curve contains a well resolved series of melting peaks (10 peaks) between 84 and 131°C suggesting that independently melting crystallites are formed during the stepwise cooling. The broad melting range indicates that LLDPE has a range of lamella thicknesses and therefore a wide distribution of branching content. Calculations show that LLDPE contains 4–21 branches per 1000 carbons (Table 2). This disperse distribution of branching is due to the multiple active sites of the catalyst used in the solution/slurry polymerisation process. Each of the peaks in the DSC curve is due to the molecules or segments of molecules of a particular distance between branches. The branches are expected to be excluded from the crystals, under the stepwise isothermal conditions used,

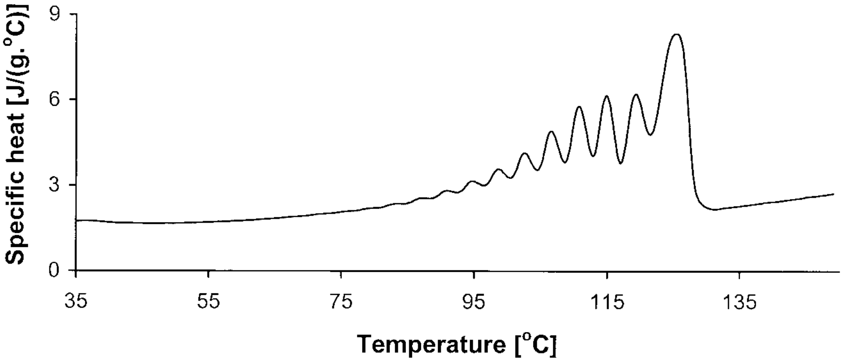

Fig. 1. DSC specific heat curve of LLDPE obtained after thermal fractionation.

thus the lamella thickness is limited by the distance between branches. It is considered that, in ethylene copolymers, branches longer than $-CH_3$ are mostly excluded from the crystal [36]. As a result, the lamella thickness and crystallinity are reduced in ethylene copolymers. The crystals under each of the peaks cannot undergo lamella-thickening growth with time and temperature due to this limitation. The crystals represented by each peak have been formed under isothermal conditions over a period of 50 min and the crystals of each subsequent peak of a lower temperature were unable to crystallise during this period when the temperature was 4°C higher. Müller et al. [37] examined LLDPE cooled under different conditions by transmission electron microscopy. They found that LLDPE, which was slowly cooled, produced a higher proportion of thicker lamella crystals with an overall higher degree of crystallinity. It was observed that thermally fractionated LLDPE also showed a higher degree of crystallinity (calculated from DSC data, Table 2) indicating that a higher proportion of thicker lamella crystals may have formed upon step-wise cooling.

The specific heat curves for thermally fractionated VLDPEs are shown in Figs. 2 and 3. The branches in these single-site catalysed VLDPEs are expected to be more evenly distributed along the molecule giving a narrower melting range than LLDPEs. VLDPE1 showed seven peaks in the temperature range of 85–120°C. The highest melting peak temperature appears at 111°C indicating that there are no unbranched sequences capable of providing higher melting temperature crystals. Most of the crystals melt in this one peak, though there is a series of smaller peaks, appearing to about 85°C, which are due to more highly branched molecules or molecular segments. However, the long branches present in VLDPE1 are not significant for determining the distribution of lamella thicknesses because they are mostly excluded from the crystal. The branching distribution in VLDPE1 varies from 10 to 21 branches per 1000 carbons.

It can be seen from Fig. 3 that VLDPE2 also exhibited nine peaks with the lowest and highest peak melting temperatures appearing at 76 and 107°C, respectively. The lowering of the melting range of VLDPE2 (85–120°C versus 73–112°C) indicates that VLDPE2 contains more branching (12–27 branches per 1000 carbons) which lowers the peak melting temperatures compared with VLDPE1. As seen in VLDPE1 specific heat curve, the majority of crystals of VLDPE2 melt in the highest melting peak at 107°C. Nonetheless, the lower melting endotherms of VLDPE2 are larger than those of VLDPE1 indicating that the distribution of branching is slightly greater in VLDPE2. The high level of branching of VLDPE2 is also supported by the efficient processability due to the improved melt rheology as shown by Swogger and co-workers [38].

Blends of copolymers were similarly analysed with a view to determine the extent to which the polymers either co-crystallise or crystallise independently. Although

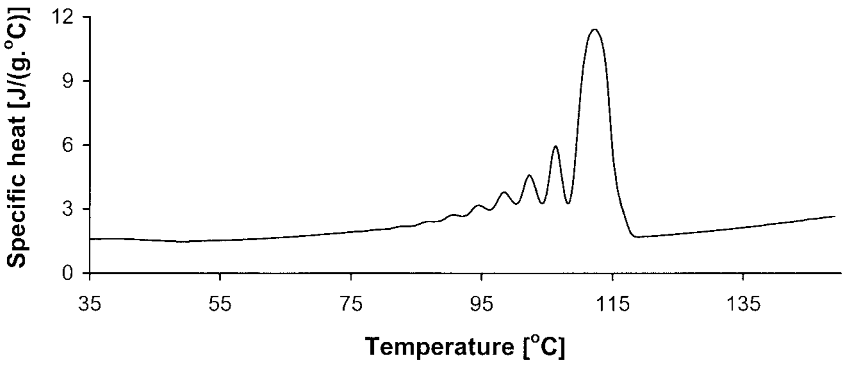

Fig. 2. DSC specific heat curve of VLDPE1 obtained after thermal fractionation.

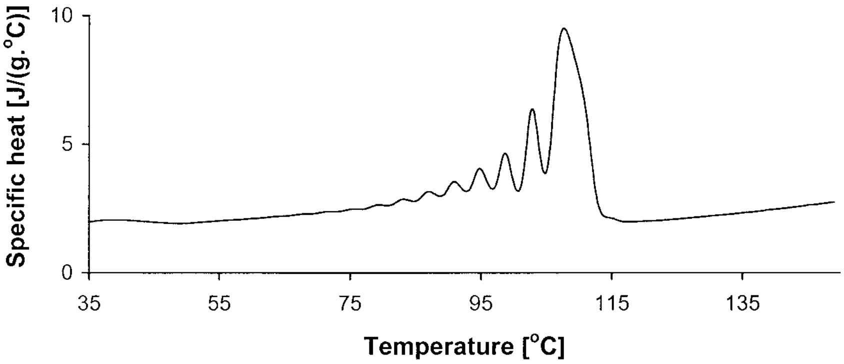

Fig. 3. DSC specific heat curve of VLDPE2 obtained after thermal fractionation.

LLDPE, VLDPE1 and VLDPE2 differ in the amount and distribution of the comonomer chemically, they should be miscible. The long branches in VLDPEs do not affect the crystallisation since there are few of them. Nonetheless, they are expected to affect the rheology and especially the melt strength. If the LLDPE and a VLDPE are miscible then they should be able to co-crystallise where the segment lengths between branches are the same in each polymer. It has been shown that more flexible *n*-alkane units can incorporate into the crystal lattice and miscibility is more likely to occur when the branching is similar [39]. Fig. 4 presents the melting of a series of blends of LLDPE with VLDPE1 after thermal fractionation; the individual polymers are shown in the top and bottom curves. Addition of VLDPE1 to LLDPE simply dilutes the larger melting peak of the LLDPE, while increasing the size of the lower series of melting peaks. Blending 20% of LLDPE to VLDPE1 separated the main melting peak of VLDPE1 into two

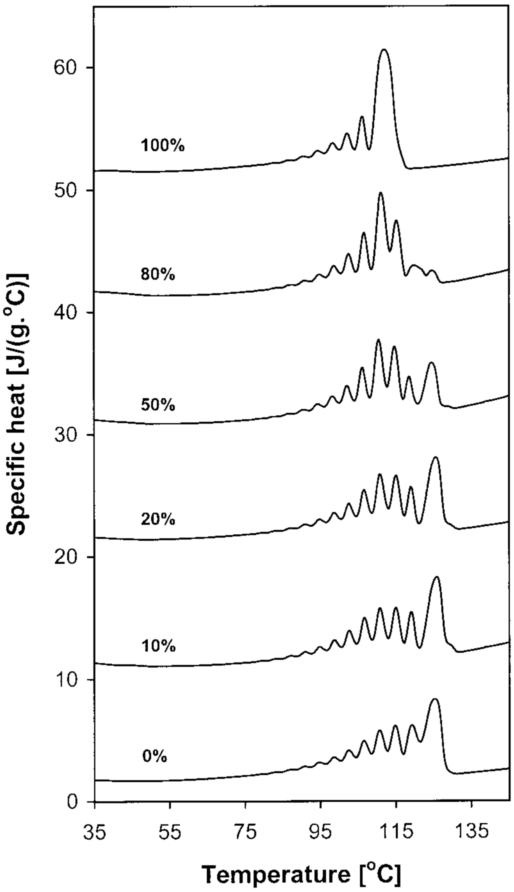

Fig. 4. Specific heat curves of LLDPE–VLDPE1 blends after thermal fractionation. An adapted scale is drawn by consecutively adding 10 units to each curve.

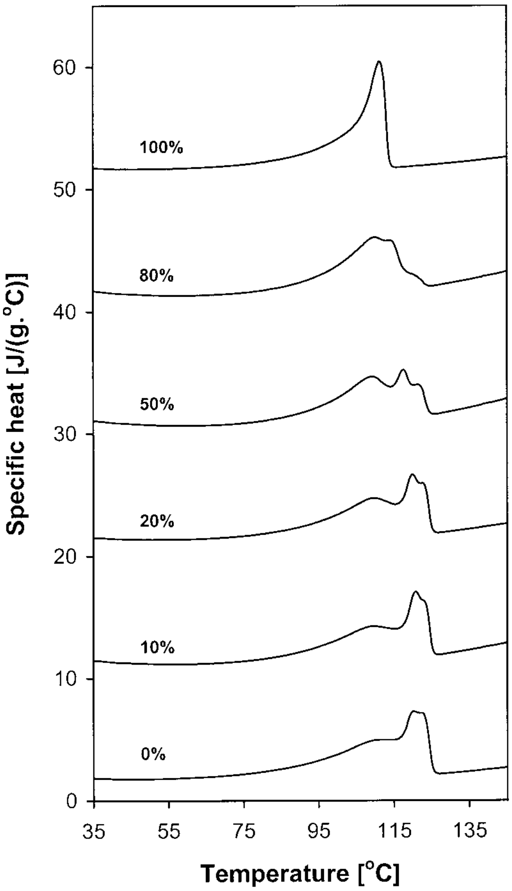

Fig. 5. Specific heat curves of LLDPE–VLDPE1 blends after cooling at 10°C/min. An adapted scale is drawn by consecutively adding 10 units to each curve.

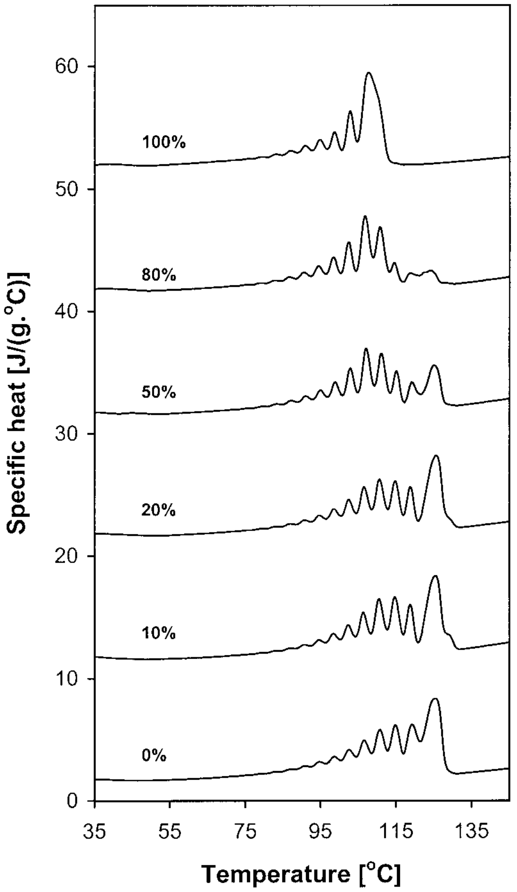

Fig. 6. Specific heat curves of LLDPE–VLDPE2 blends after thermal fractionation. An adapted scale is drawn by consecutively adding 10 units to each curve.

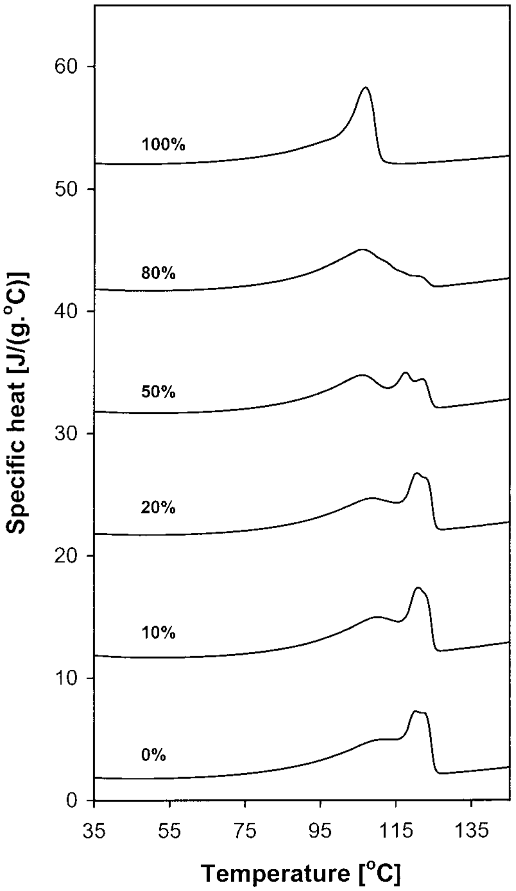

Fig. 7. Specific heat curves of LLDPE–VLDPE2 blends after cooling at 10°C/min. An adapted scale is drawn by consecutively adding 10 units to each curve.

sharper peaks. The main melting peak of VLDPE1 was broad though not resolved in the pure polymer. These changes indicate that there must be some co-crystallisation between the two polymers in the 80% VLDPE1 blend.

Fig. 5 contains the DSC specific heat curves for the same series of blends after cooling from the melt at 10°C/min and the peak melting temperatures associated with them are listed in Table 3. The presence of multiple-peaked crystallisation and melting curves was observed for copolymers and their blends. These results are characteristic of intermolecular heterogeneity [16]. As mentioned before, the multiple-peaked DSC specific

Table 3
Crystallisation and melting characteristics of pure polymers and their blends at scanning rates of 10°C/min

Polymers and blends	$T_m'^{a}$ (°C)	ΔH_m (total) (J/g)	T_c^{b} (°C)	ΔH_c (total) (J/g)
LLDPE	120	9.9	106	11.5
VLDPE1	111	9.3	97	10.9
VLDPE2	107	7.9	91	9.4
10% VLDPE1	121	8.4	107	11.4
20% VLDPE1	120	9.0	106	11.8
50% VLDPE1	118	8.0	104	11.4
80% VLDPE1	110	8.0	101	11.2
10% VLDPE2	121	9.2	107	11.8
20% VLDPE2	120	9.0	107	11.4
50% VLDPE2	118	7.9	107	11.0
80% VLDPE2	106	7.4	97	10.0

[a] Multiple melting peaks were observed for LLDPE and all blends. The value of the highest melting peak is reported.

[b] Cooling curves had shoulder on low-temperature side.

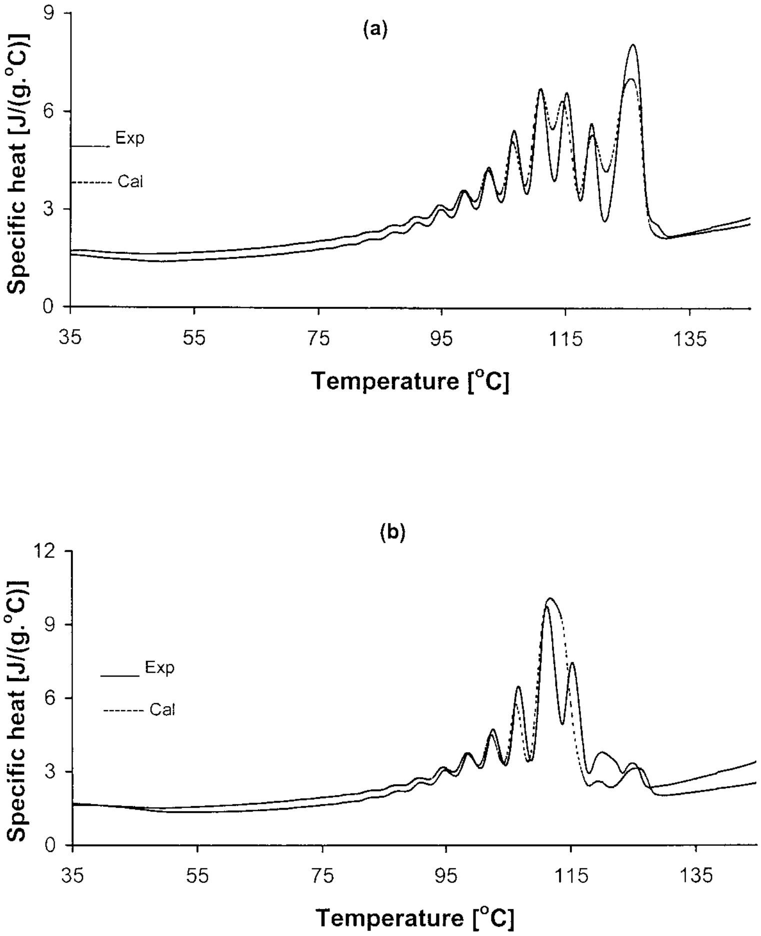

Fig. 8. Comparison of experimental and calculated specific heat curves of LLDPE–VLDPE1 blends after thermal fractionation: (a) 20% VLDPE1; (b) 80% VLDPE1 blends.

heat curve of LLDPE (bottom curve) is an indication of heterogeneous comonomer incorporation in LLDPE. The higher melting peaks due to LLDPE stay at the same temperature but are diluted by VLDPE1. The lower melting peak of VLDPE1 and LLDPE are at the same temperature, though that of LLDPE is much broader. This lower melting peak temperature decreases slightly to a minimum for the 50% VLDPE1 blend. Again co-crystallisation between some of the LLDPE and VLDPE1 in this range of branching compositions may take place. Moreover, it is seen that the information provided in these curves is limited compared with those of thermally fractionated blends.

Fig. 6 shows the melting of a series of blends of LLDPE and VLDPE2 after thermal fractionation. Similar observations to those for the blends of LLDPE and VLDPE1 are apparent, though the temperature range for the changes due to co-crystallisation are decreased due to the lower melting temperature of VLDPE2. A small peak appeared on the high temperature side of the main melting peak of LLDPE in 10 and 20% VLDPE2 blends. The splitting of the high temperature peak of VLDPE2 into two peaks is again observed in the 80% VLDPE2 blend. The presence of LLDPE has enabled the crystallisation of VLDPE2 to be better resolved in this temperature range.

The DSC curves obtained after cooling at 10°C/min are shown in Fig. 7. Again, these curves present less detail about the crystallisation of the blends. The broad lower temperature melting peak, due to VLDPE2 and part of the LLDPE decreased slightly for the 20, 50 and 80% VLDPE2 blends, indicating that some co-crystallisation has occurred in this melting range. The higher melting temperature peak, due to LLDPE, stayed at the same temperature, while the middle melting peak, also due to the LLDPE decreased markedly for the 50% VLDPE2 blend.

In order to better observe the effects of additivity on the melting of the blends calculated specific heat curves were obtained for the blends. The specific heat curves for the pure polymers after thermal fractionation were added in the fraction each was present in the blend to provide a calculated specific heat curve for the blends. Only the curves for the 20 and 80% VLDPEs are shown, since these show the greatest change and illustrate the procedure. The use of specific heat curves for the DSC results has enabled this procedure to be used since heat flow curves only provide relative DSC

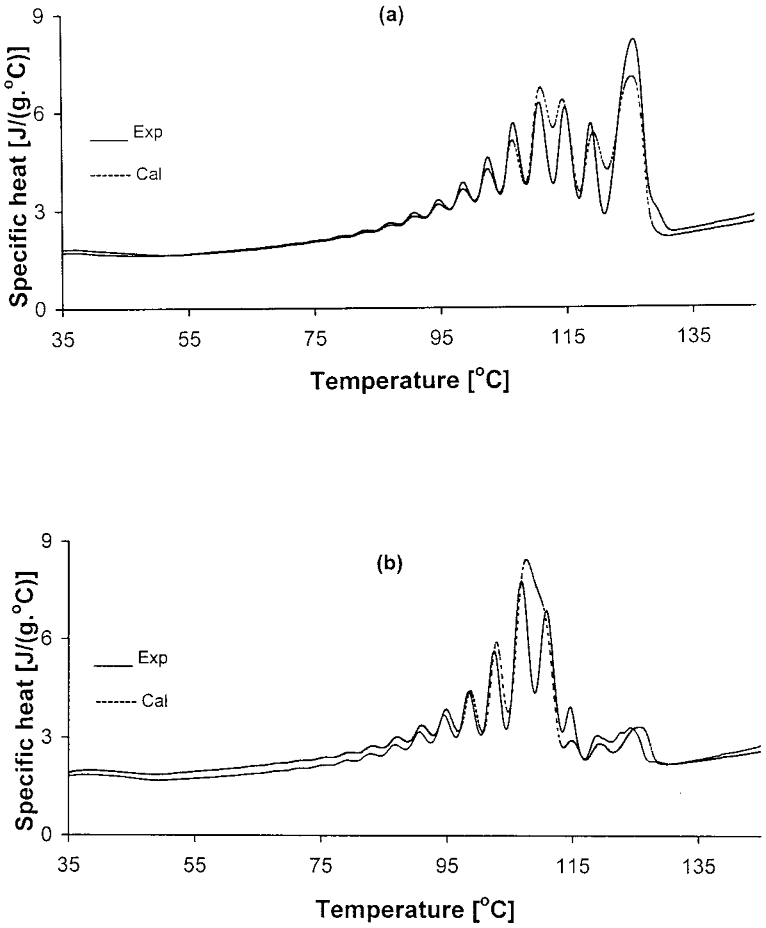

Fig. 9. Comparison of experimental and calculated specific heat curves of LLDPE–VLDPE2 blends after thermal fractionation: (a) 20% VLDPE2; (b) 80% VLDPE2 blends.

curves. Even when the heat flow curves are normalised for the mass of the sample the heat flow scan is relative since the zero line in not known. The specific heat curves provide an absolute representation of DSC data, with the zero line being a true zero and the baseline of the polymer representing the specific heat of the polymer at any temperature along the curve. Generally, the specific heat of polyethylene is about 2 J/(g °C).

The calculated and observed specific heat curves for VLDPE1 and VLDPE2 blends are shown in Figs. 8 and 9. A close match is seen between the calculated and observed curves of 20% VLDPE1 blend (see Fig. 8(a)), except that the experimental curve shows better fractionation resolution at 120 and 112°C, and the greater intensity of the highest melting peak. Apart from these changes the two polymers could be considered to have crystallised separately. The 80% VLDPE1 blend shows greater differences between the calculated and observed curves in the region where VLDPE1 has its main melting peaks. The calculated curve displays a broad main melting peak for VLDPE1, whereas the observed curve contains two resolved peaks for the same temperature range. Furthermore, the two highest temperature peaks, due to the LLDPE have changed relative areas with the second highest peak being larger in the observed curve. The peak at 107°C is also larger in the observed curve. In the 80% VLDPE1 curves, these differences indicated that the two polymers are having an effect on their crystallisation in the blend. This suggests that they are miscible or partially miscible and are able to co-crystallise. Similar behaviour was observed for VLDPE2 blends. The 20% VLDPE2 blend shows very good agreement between the calculated and observed curves, and in this case the calculated curve again shows less fractionation resolution. The curves for the 80% VLDPE2 blend display changes in the same regions as described above.

Crystallisation is very selective even within the one polyethylene. If the LLDPE and VLDPE are immiscible in the melt near the temperature of crystallisation they will crystallise essentially independently. If they are miscible in the melt they may still crystallise independently, since crystallisation is very selective about structure. If they are miscible in the melt and, in part, co-crystallise then the morphology of the LLDPE will be changed. They are only expected to co-crystallise when they have similar unbranched segment lengths. Small differences in the branching between polyethylenes also results in liquid–liquid phase separation.

Further studies will be carried out to investigate the microstructures and phase behaviour of these blends in the melt.

4. Conclusion

Thermal fractionation by DSC separates copolymers according to their branching densities so that thermal fractionation data was used to calculate branching distribution in polyethylenes using calibration curves obtained by TREF data. It is found that many branches are present in the octene LLDPE studied and the branch content of this copolymer varies from 4–21 branches per 1000 carbons. VLDPEs, contained a narrow distribution, though with shorter average lengths between branches. Since the total specific heat of the 10 and 20% VLDPE blends appears to follow the additivity rule, the ability of LLDPE to crystallise is not prevented by the VLDPE or vice versa. The blends with high VLDPE amounts show some miscibility in the melt indicating that there may be cocrystallisation between copolymers. Thermal fractionation of polymers can be performed using a DSC and is useful in characterisation of copolymers and their blends.

Acknowledgements

We wish to thank Dr Kate Drummond, Corporative Research Centre for Polymers for the helpful discussions and assistance given in the preparation of manuscript.

References

[1] Utracki LA. Polymer alloys and blends: thermodynamics and rheology, New York: Hanser, 1989.
[2] Bibee DV, Dohrer KK. TAPPI Proc 1987:639.
[3] Speed CS. Plast Eng 1982;July:39.
[4] Swogger KW. Second Int Business Forum Proc 1992:155.
[5] Knight GW, Lai S. Eighth Int Polyolefins Conf Proc 1993:226.
[6] Leaversuch RD. Mod Plastic Int 1997;December:27.
[7] Neves CJ, Monteiro E, Habert AC. J Appl Polym Sci 1995;50:817.
[8] Defoor F, Groeninckx G, Reynaers H, Schouterden P, Van der Heijden B. J Appl Polym Sci 1993;47:1839.
[9] Wild L, Ryle TR, Knobleloch DC, Peat IR. J Polym Sci, Phys Ed 1982;20:441.
[10] Hosada S. Polym J 1988;20:383.
[11] Barbalata A, Bohossian T, Delmas G. J Appl Polym Sci 1992;46:411.
[12] Karbashewski E, Kale L, Rudin A, Tchir WJ, Cook DG, Pronovost JO. J Appl Polym Sci 1992;44:425.
[13] Hsieh ET, Tso CC, Byers JD, Johnson TW, Fu Q, Cheng SD. J Macromol Sci—Phys 1997;B36:615.
[14] Feng Y, Jin X. Polym Plast Tech Engng 1998;37:271.
[15] Donatelli AA. J Appl Polym Sci 1979;23:3071.
[16] Mathot VBF. Calorimetry and thermal analysis of polymers, New York: Hanser, 1993 chap. 9.
[17] Fu Q, Chiu FC, McCreight KW, Guo M, Tseng WW, Cheng SZD, Keating MY, Heish ET, DesLauriers P. J Macromol Sci—Phys 1997;B36:41.
[18] Zhou X, Hay JN. Eur Polym J 1993;29:291.
[19] Woo L, Westphal SP, Ling TK, Khare AR. Polym Preprints 1998;39:203.
[20] Varga J, Menczel J, Solti A. J Thermal Anal 1979;17:333.
[21] Kamiya T, Ishikawa N, Kambe S, Ikegami N, Nishibu H, Hattori T. Soc Plast Engng ANTEC Proc 1990:871.
[22] Wolf B, Kenig S, Klopstock J, Miltz J. J Appl Polym Sci 1996;62:1339.
[23] Balbontin G, Camurati L, Dall'Occo T, Finotti A, Franzese R, Vecellio G. Angew Makromol Chem 1994;219:139.
[24] Balbontin G, Camurati L, Dall'Occo T, Zeigler R. J Mol Catalyst A: Chemical 1995;98:123.
[25] Adisson E, Ribeiro M, Deffieux A, Fontanille M. Polymer 1992;33:4337.
[26] Shanks RA, Drummond KM. ANTEC Proc 1998:2004.
[27] Zhang M, Huang J, Lynch D, Wanke SE. ANTEC Proc 1998:539.
[28] Keating MY, McCord EF. Thermochim Acta 1994;243:129.
[29] Chiu FC, Keating MY, Cheng SZD. ANTEC Proc 1995:1503.
[30] Keating MY, Lee I-H, Wong CS. Thermochim Acta 1996;284:47.
[31] Starck P. Polym Int 1996;40:111.
[32] Müller AJ, Heránndez ZH, Arnal ML, Sánchez JJ. Polym Bull 1997;39:465.
[33] Arnal ML, Heránndez ZH, Matos M, Sánchez JJ, Méndez G, Sánchez A, Müller AJ. ANTEC Proc 1998:611.
[34] Arnal ML, Sánchez JJ, Müller AJ. ANTEC Proc 1999:2329.
[35] Flory PJ. Trans Faraday Soc 1955;51:848.
[36] Voigt-Martin IG, Alamo R, Mandelkern L. J Polym Sci, Polym Phys Ed 1986;24:1283.
[37] Balsamo V, Müller AJ. J Mater Sci Lett 1993;12:1457.
[38] Swogger KW, Lancaster GM, Lai SY, Butler TI. J Plastic Film Sheeting 1995;11:102.
[39] Zhou X, Hay JN. Polymer 1993;34:1002.